A Conceptual Model of a Shallow Circulation Induced by Prescribed Low-Level Radiative Cooling

ANN KRISTIN NAUMANN, BJORN STEVENS, CATHY HOHENEGGER, AND JUAN PEDRO MELLADO

Max Planck Institute for Meteorology, Hamburg, Germany

(Manuscript received 31 January 2017, in final form 28 June 2017)

ABSTRACT

A conceptual bulk model for a dry, convective boundary layer with prescribed horizontally homogeneous and heterogeneous low-level radiative cooling rates is developed. For horizontally homogeneous radiative cooling, the response of the system to varying its prescribed parameters is explored and formulated in terms of nondimensional parameters. Large-eddy simulations with prescribed radiative cooling rates match the results of the bulk model well. It is found that, depending on the strength of the surface coupling, the height of the boundary layer (BL) either increases or decreases in response to increasing radiative BL cooling. Another property of the system is that, for increasing surface temperature, the BL temperature decreases if the prescribed radiative BL cooling rates are strong. This counterintuitive behavior is caused by the formulation of the entrainment rate at the inversion. Heterogeneous radiative BL cooling is found to cause a circulation induced by pressure deviations between the area of weak radiative BL cooling and the area of strong radiative BL cooling. Including the feedback of the induced circulation on the BL in a two-column model leads to a modified equilibrium state, in which a weakened horizontal BL flow of about 1 m s^{-1} is maintained for differences in radiative BL cooling rates larger than 1 K day^{-1}. Such a circulation strength is comparable to a shallow circulation caused by surface temperature differences of a few kelvins. Spatial differences in radiative BL cooling should therefore be considered as a first-order effect for the formation of shallow circulations.

1. Introduction

In numerical simulations of radiative convective equilibrium (RCE), convection can aggregate by spontaneous clustering of randomly distributed convective cells into organized mesoscale convection despite homogeneous boundary conditions (e.g., Held et al. 1993; Bretherton et al. 2005). This self-aggregation occurs under a wide range of circumstances: coupled or fixed surface boundary conditions, explicit or parameterized convection, and different model domain sizes and resolutions (e.g., Muller and Held 2012; Coppin and Bony 2015; Hohenegger and Stevens 2016). Various mechanisms have been proposed to initiate, maintain, or counteract self-aggregation (Bretherton et al. 2005; Muller and Held 2012; Craig and Mack 2013; Jeevanjee and Romps 2013; Wing and Emanuel 2013; Emanuel et al. 2014; Coppin and Bony 2015; Holloway and Woolnough 2016). One of these is a low-level radiative cooling–circulation feedback: A circulation induced by low-level radiative cooling transports moist static energy upgradient from dry, nonconvective areas into moist, convective areas,[1] thereby acting as a positive feedback (Fig. 1, left and middle; Bretherton et al. 2005; Muller and Held 2012; Wing and Emanuel 2013; Muller and Bony 2015). In this study, we investigate how low-level radiative cooling in nonconvecting areas affects the boundary layer (BL) structure and its dynamics. To do so, we develop a conceptual model with prescribed radiative cooling rates and analyze the resulting circulation.

In RCE simulations of organized convection, the BL structure differs between the convective and the nonconvective regions. Radiation profiles show strong longwave radiative cooling rates near the BL top of the nonconvective region because the free troposphere (FT) dries as a result of subsidence, which leads to small

[1] We adopt the terminology used in RCE modeling studies where ''convective areas'' include deep convective cells that organize into mesoscale clusters, and in ''nonconvective areas'' deep convection is suppressed by subsidence, but shallow clouds might still be present.

Corresponding author: Ann Kristin Naumann, ann-kristin.naumann@mpimet.mpg.de

DOI: 10.1175/JAS-D-17-0030.1

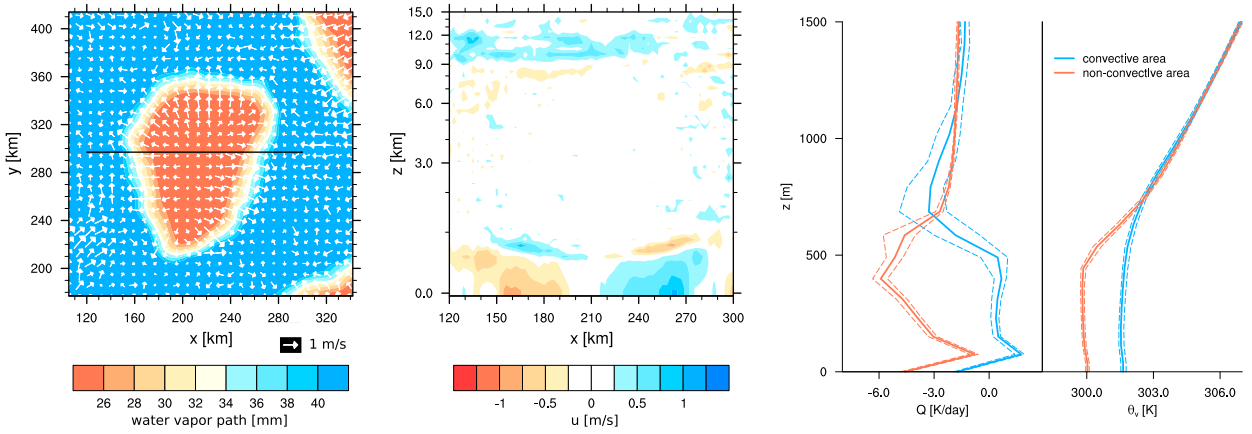

FIG. 1. The BL structure from an RCE simulation with 3-km grid spacing. (left) Water vapor path and surface wind in a subset of the domain at the onset of aggregation. (middle) The x component of the wind vector at the cross section indicated in the left panel. (right) Profiles of the net radiative cooling rate Q and the virtual potential temperature θ_v in the aggregated state. Solid lines show time averages for 1 day; dashed lines show the minimum and maximum of snapshots from that day. The mean radiative BL cooling Q_{BL} in the nonconvective area is approximately -4 K day^{-1} and in the convective area approximately 0 K day^{-1}. The data correspond to the simulation named U500 from Hohenegger and Stevens (2016), in which the SST is calculated interactively from an ocean mixed-layer model with 500-m depth. Because the ocean mixed layer is deep, the SST is almost homogeneous in the domain with a value of 301 K.

downward longwave radiative fluxes. The longwave cooling of the BL is offset only partially by shortwave radiation and results in a net radiative cooling rate of several kelvins per day (Fig. 1, right). In the nonconvective region, the BL is shallower, and its temperature is lower than in the convective region. Dynamically, the BL is characterized by near-surface winds from the nonconvective region to the convective region on the order of a meter per second, both at the onset of aggregation (Fig. 1, left) and in the aggregated state (Hohenegger and Stevens 2016, Fig. 1 therein). Just above the BL top, a return flow develops, which, together with the near-surface wind, forms a shallow circulation (Fig. 1, middle). This shallow circulation is superimposed on the primary, deep circulation associated with deep convection and transports moist static energy into the energy-rich, convecting regions, thus supporting convection. Particularly on large scales, this raises the question as to what extent radiative processes in the lower nonconvecting atmosphere are important in determining the structure of regions of deep convection.

In addition to the idealized RCE simulations, a secondary, shallow circulation is also observed and modeled in the vicinity of the intertropical convergence zone (ITCZ) (e.g., Trenberth et al. 2000; Zhang et al. 2008). A shallow meridional circulation is superimposed on the Hadley cell, with the descending branch in the subsidence regions of the subtropics, the ascending branch in the ITCZ, and horizontal flows connecting the branches near the surface and just above the BL. Three mechanisms are proposed to cause a shallow meridional circulation over tropical oceans: strong sea surface temperature gradients, which induce a sea breeze (Nolan et al. 2007), shallow convection in subsiding regions and the associated latent heating (Wu 2003), and radiative cooling at the BL top in subsiding regions due to a dry FT (Wang et al. 2005; Nishant et al. 2016). Both surface temperature gradients and radiative cooling at the BL top can enhance precipitation in the ITCZ region by up to 20% (Wang et al. 2005; Sobel and Neelin 2006). In addition, surface temperature gradients are also known to affect pressure gradients in the tropics, BL convergence, and thereby the strength of the ITCZ (e.g., Lindzen and Nigam 1987; Neelin and Held 1987; Sobel and Neelin 2006; Back and Bretherton 2009; Fermepin and Bony 2014). Shallow convection has been shown to influence the ITCZ and tropical cyclone tracks (Tiedtke et al. 1988; Neggers et al. 2007; Torn and Davis 2012). However, those arguments do not rule out an important role of radiatively driven low-level circulations, because both surface temperature gradients and shallow convection can strongly influence radiative cooling rates in the subsidence regions and vice versa (Nishant et al. 2016).

Interpretation of the role of shallow circulations has been advanced by several conceptual studies: Nicholls et al. (1991), Wu et al. (2000), and Wu (2003) show how heat sources and sinks induce vertical motion and horizontal circulation and that a surface circulation can be driven by a shallow heat source and not by an elevated heat source above the BL top. In two-column models, large-scale, deep circulation arises from

radiative–convective feedbacks with and without surface temperature gradients (Pierrehumbert 1995; Nilsson and Emanuel 1999; Raymond and Zeng 2000). Analyzing the interplay between radiation, moisture, and convection, Emanuel et al. (2014) and Beucler and Cronin (2016) find that instabilities, which correspond to the self-aggregation of convection, depend on the vertical structure of water vapor and are favored for high BL humidity.

In a stably stratified fluid and in the absence of other diabatic heat sources or sinks, radiative cooling is to a good approximation balanced by subsidence warming. This balance accounts for the weak temperature gradients in the tropical FT and is used as an assumption in many models (Sobel and Bretherton 2000). If radiative cooling is concentrated in a well-mixed BL, as is typical in the BL over tropical oceans, the weak temperature gradient approximation is not valid and the dynamical response of the flow is less clear. The lack of stratification in the BL implies that radiative cooling cannot be balanced by warming due to vertical motion but must be balanced by other processes, such as surface fluxes or entrainment at the inversion.

In this study, we aim to understand to what extent low-level radiative cooling drives subsidence and a circulation in the BL. We develop a conceptual bulk model that applies the weak temperature gradient approximation in the FT, and for the BL assumes a balance of radiative cooling, surface fluxes, and entrainment at the inversion. The flux-jump relation is used to describe entrainment across the inversion at the BL top (Ball 1960; Deardorff et al. 1969) and this entrainment is then expressed as a fraction of the surface flux (e.g., Stevens 2006). Without subsidence from above, the standard dry convective BL bulk model describes the growth of the BL in time. With subsidence in the FT, the deepening of the BL can be balanced, and an equilibrium state of the BL is reached. This equilibrium depends on the strength of the radiative BL cooling, the surface temperature, and the stratification in the FT. For a horizontally heterogeneous radiative cooling in the BL (such as in the convective and the nonconvective areas of Fig. 1), different equilibrium states will be reached, which causes a pressure difference that leads to a compensating circulation.

We use a conceptual model to explore the link between low-level radiative cooling, surface forcing, BL properties, and such a circulation. How effective is radiative BL cooling vis a vis surface temperature changes in changing BL properties? Does horizontally heterogeneous radiative cooling in the BL induce a shallow circulation? And if so, how does the strength of such a circulation depend on the radiative cooling rate? The findings can then be used as an interpretative framework for understanding the role of radiative cooling in nonconvective areas for the structure of convection. In this study, we focus on the case of the dry BL. The basic dynamics that our model illustrates is important for the interpretation of the response of moist flows, including links to regions of deep convection, but the explicit consideration of moisture effects will be taken up in a future study.

The rest of the paper is structured as follows: In section 2, we develop and analyze a conceptual model for horizontally homogeneous radiative cooling and compare its equilibrium state to large-eddy simulations (LES). In section 3, we extend this conceptual model to the case of heterogeneous radiative cooling and analyze the induced horizontal flow and its feedback on the BL. Finally, in section 4, we give some concluding remarks.

2. A bulk model for horizontally homogeneous radiative cooling

The conceptual bulk model developed in this section represents a region characterized by subsidence in the FT, w_{FT}, which dries the FT, sharpens the BL inversion, and allows for strong radiative cooling from the BL (Fig. 2). It is akin to the situation encountered in nonconvective areas of organized convection. In analogy to Fig. 1, we prescribe distinct radiative cooling rates both in the BL and in the FT, Q_{BL} and Q_{FT}, respectively. We formulate the bulk model in terms of a dry, convective BL and analyze the response of the BL to prescribed changes in Q_{BL}. Besides the radiative cooling rates, the temperature profile in the FT, θ_{FT}, as well as the surface temperature θ_{sfc} are prescribed.

a. *Formulation of the basic equations and comparison with LES*

We assume that the system is in equilibrium and that the BL is well mixed so that the potential temperature in the BL, θ_{BL}, is constant with height. Then the budget equations are as follows (e.g., Stevens 2006):

$$\frac{\partial \theta_{\mathrm{BL}}}{\partial t} = Q_{\mathrm{BL}} + \frac{1}{h}(w_e \Delta\theta + F_\theta) = 0, \tag{1}$$

$$\frac{\partial \theta_{\mathrm{FT}}}{\partial t} = Q_{\mathrm{FT}} - \Gamma w_{\mathrm{FT}} = 0, \quad \text{and} \tag{2}$$

$$\frac{\partial h}{\partial t} = w_e + w_{\mathrm{FT}} = 0. \tag{3}$$

Here, h is the BL height, w_e the entrainment velocity at the inversion, F_θ the kinematic surface heat flux, and $\Gamma = \partial\theta_{\mathrm{FT}}/\partial z$ the temperature gradient in the FT.

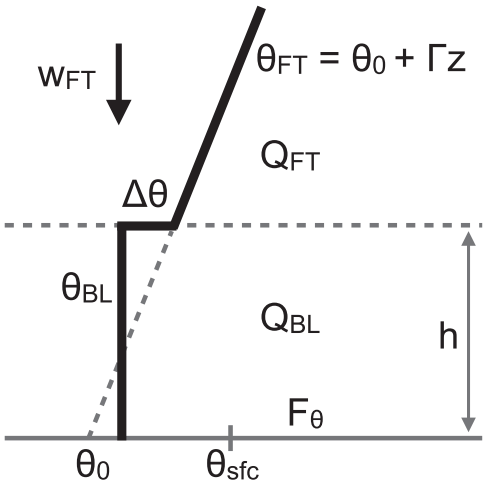

FIG. 2. Sketch of the bulk model with some characteristic variables. See text for explanation of the variables.

The inversion strength $\Delta\theta$ is defined as the temperature jump at the inversion:

$$\Delta\theta = \theta_0 + \Gamma h - \theta_{BL}, \tag{4}$$

where θ_0 is a reference surface temperature to determine $\theta_{FT}(z \geq h) = \theta_0 + \Gamma z$. Equation (1) applies the flux-jump relation; that is, it is assumed that the kinematic vertical heat flux at the inversion is related to the product of the entrainment velocity and the temperature jump at the inversion ($\overline{w'\theta'}_h = -w_e\Delta\theta$; Ball 1960; Deardorff et al. 1969). Equation (2) expresses the weak temperature gradient assumption (Sobel and Bretherton 2000), which is valid in the FT but not in the BL (see Fig. 1, right).

Additionally, we apply two closure assumptions that are often applied in bulk models of a dry convective boundary layer (e.g., Stevens 2006):

$$w_e = \frac{AF_\theta}{\Delta\theta} \quad \text{and} \tag{5}$$

$$F_\theta = C_d V(\theta_{sfc} - \theta_{BL}). \tag{6}$$

The inversion entrainment efficiency A in Eq. (5) is determined by the flow. We fix A on the basis of LES (setup described below) as discussed by Deardorff et al. (1974): instead of employing the entrainment flux minimum influenced by the gradual inversion in the LES, we interpolate to a minimum value that would emerge in the case of a temperature jump at the inversion as it is assumed in the conceptual model. The derivation and physical interpretation of A is discussed by Garcia and Mellado (2014), and the sensitivity of BL properties on the value of A has been studied, for example, by van Heerwaarden et al. (2009). The second closure equation, Eq. (6), is a simple bulk aerodynamic law formulation of the surface heat flux with C_d being the drag coefficient and V the background wind speed, which can be associated with a large-scale circulation, for example, caused by deep convective regions. The surface velocity scale $C_dV = F_\theta/(\theta_{sfc} - \theta_{BL})$ has the same order of magnitude as w_e.

TABLE 1. Prescribed parameters used in this study if not explicitly stated otherwise. Parameters in the top eight rows are introduced in section 2; parameters in the bottom two rows are introduced in section 3.

Parameter	Value
Q_{BL}	-1.0 to -6.0 K day^{-1}
Q_{FT}	-1.0 K day^{-1}
Γ	5.0 K km^{-1}
θ_0	298.0 K
θ_{sfc}	301.0 K
A	0.41
C_d	0.001
V	5 m s^{-1}
X_p	20 km
$X_1 = X_2$	100 km

Prescribing seven parameters (Q_{BL}, Q_{FT}, Γ, θ_0, θ_{sfc}, A, and C_dV), these six equations [Eqs. (1)–(6)] yield a closed system and can be solved for six variables: h, θ_{BL}, $\Delta\theta$, F_θ, w_e, and w_{FT}. To gain some insight into the behavior of the bulk model, we first set all parameters constant except for Q_{BL}. The values of the parameters are set to approximately resemble the state of organized convection, except for A, which is fixed on the basis of LES of the dry convective boundary layer (Table 1). According to the weak temperature gradient assumption [Eq. (2)] and the equilibrium of the BL height [Eq. (3)], w_{FT} and w_e are then also constant. With the parameter values in Table 1, $w_{FT} = -w_e = -0.0023\,\text{m s}^{-1}$, where both vertical velocities are defined positive upward. The other four variables (h, θ_{BL}, $\Delta\theta$, and F_θ) change with Q_{BL}.

With stronger radiative BL cooling (i.e., more negative Q_{BL}), θ_{BL} decreases (Fig. 3). A decrease in θ_{BL} causes an increase in F_θ and an increase in $\Delta\theta$. In equilibrium, the changes in F_θ and $\Delta\theta$ are proportional to each other because w_e is kept constant [Eqs. (3) and (5)]. The response of h to a change in radiative BL cooling is more intricate. A negative perturbation in Q_{BL} or θ_{BL} perturbs w_e both through an increase in F_θ and in $\Delta\theta$. Depending on whether the effect of F_θ or $\Delta\theta$ dominates, h increases or decreases until an equilibrium is reached, in which w_e returns to its original value before the perturbation, that is, equal to w_{FT} [Eq. (3)]. For the set of parameters given in Table 1, stronger radiative BL cooling results in a decrease in h in equilibrium. We will show later that, for a different

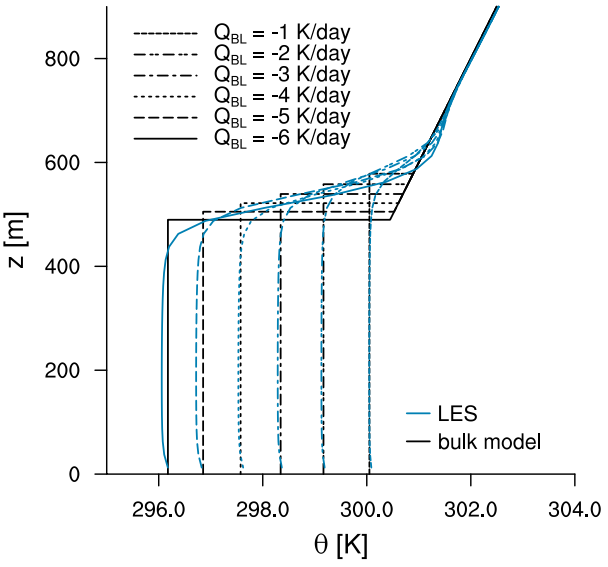

FIG. 3. Temperature profiles as a function of radiative BL cooling from the bulk model (black) and the LES (blue). Prescribed parameters are given in Table 1.

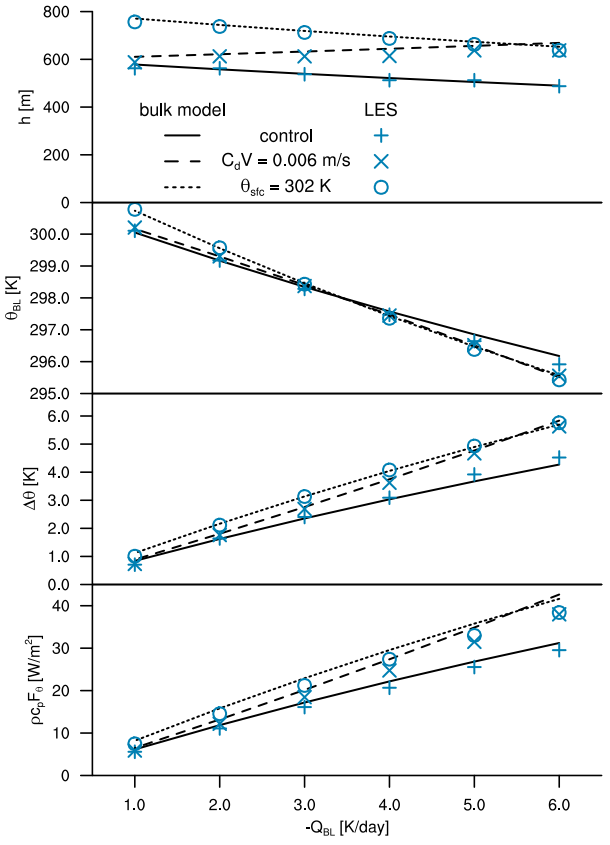

FIG. 4. The BL properties as a function of radiative BL cooling from the bulk model (lines) and the LES (markers). The control case uses the prescribed parameters given in Table 1 (i.e., C_dV = 0.005 m s^{-1} and θ_{sfc} = 301 K) and corresponds to the profiles shown in Fig. 3. For the other two cases, all parameters are the same, but either C_dV or θ_{sfc} is increased.

set of parameter values, h can also increase with stronger radiative BL cooling.

The results of the bulk model agree very well with results from LES, both in their absolute values and in their response to changing the prescribed parameters (Fig. 3, also Fig. 4). To conduct such a comparison, we run the University of California, Los Angeles, LES (UCLA-LES) (Stevens et al. 2005; Stevens 2007) with horizontally homogeneous, prescribed radiative cooling in the BL and the FT. The BL height is diagnosed interactively as the height of maximum temperature variance and the radiative cooling rates are adapted accordingly for each time step. The LES is used in a simplified setup to match the input parameters of the bulk model: 1) for the surface flux we use Eq. (6) with a fixed C_dV value as in the bulk model and apply the temperature difference between the first model level and the surface to approximate a value for $(\theta_{sfc} - \theta_{BL})$; 2) we apply the weak temperature gradient approximation in the FT (Sobel and Bretherton 2000) by adding a subsidence velocity in the temperature equation. In the BL, we let the subsidence velocity decrease linearly from its FT value at the inversion height to zero at the surface. This allows us to include the effect of subsidence warming in the FT and at the inversion in a consistent manner while the effect in the BL is small. Three-dimensional simulations are performed with horizontal grid spacing of 50 m, vertical grid spacing of 25 m below 2000 m, and a vertically stretched grid above. Domain size is 6.4 km × 6.4 km in the horizontal and 5.5 km in the vertical. Simulations are run for 10 days, that is, for a few more days after equilibrium is reached (usually after 7 days). The model output is averaged over the last simulation day.

The good agreement between the bulk model and the LES confirms that the ansatz of our mixed-layer model captures all processes important for the equilibrium state of the BL. It also suggests that the closure assumption for the entrainment velocity [Eq. (5)] works well because one fixed value for A is sufficient to reproduce agreement for a range of parameters (here, in particular, Q_{BL}). This allows us to extend the bulk model to analyze a circulation induced by horizontally heterogeneous radiative BL cooling in section 3. Before we do so, we now highlight some more general features of the bulk model with horizontally homogeneous radiative cooling. We also derive a non-dimensional formulation that identifies the essential parameters of the conceptual model and provides a general parameterization for any combination of parameters in the BL and in the FT.

b. General properties of the bulk model

The values and rates of change of the four variables (h, θ_{BL}, $\Delta\theta$, and F_θ) with radiative BL cooling depend on all prescribed parameters given in Table 1. In the following, we will focus on the effect of changes in C_dV (surface coupling) and θ_{sfc} (surface warming) and then discuss the results in terms of different temperature regimes.

1) Surface coupling

According to Eq. (6), C_dV describes the response of F_θ to a temperature difference between the surface and the BL; that is, larger C_dV correspond to a stronger coupling to the surface. A typical value for C_d is 0.001 and for V is 5 m s^{-1}. Therefore, an increase in C_dV can be interpreted as stronger surface coupling due to an increase in background wind speed V or due to an increase in surface roughness, expressed in terms of C_d. As expected, both the bulk model and the LES show an increase of F_θ with increasing C_dV, which becomes more pronounced for stronger radiative BL cooling (Fig. 4).

Unexpectedly, the strength of the surface coupling affects the response of h to Q_{BL} and can lead to either increasing or decreasing h with stronger radiative BL cooling depending on the value of C_dV. This is due to dependencies between F_θ, Q_{BL}, and h. Inserting Eq. (5) into Eq. (1) gives $h = -(1 + A)F_\theta/Q_{BL}$. Therefore, the change of the BL height depends on how fast the surface flux changes with increasing radiative BL cooling, which depends on the surface coupling as measured by C_dV. If F_θ increases faster than the magnitude of Q_{BL}, h increases; but if F_θ increases less rapidly than the magnitude of Q_{BL}, h decreases.

Analytically, this behavior can be understood by solving Eqs. (1)–(6) for h, which gives

$$h = \frac{\frac{\theta_{sfc} - \theta_0}{\Gamma}}{1 - \frac{Q_{BL}}{(A+1)C_dV\Gamma} - \frac{A}{A+1}\frac{Q_{BL}}{Q_{FT}}}. \quad (7)$$

Differentiating Eq. (7) with respect to Q_{BL}, one can show that $\partial h/\partial Q_{BL} = 0$ for a threshold of $C_dV_{thres} = -Q_{FT}/(A\Gamma)$ ($=0.0056$ m s^{-1} for the parameters given in Table 1). Below this threshold, h decreases with stronger radiative BL cooling (Fig. 5, top) and the decrease is strongest for $C_dV \approx 0.003$ m s^{-1}. Above C_dV_{thres}, h increases for stronger radiative BL cooling.

Physically, we can explain this behavior as follows. A negative perturbation in Q_{BL} causes a negative perturbation in θ_{BL}, and both F_θ and $\Delta\theta$ increase. If F_θ increases faster than $\Delta\theta$, w_e [Eq. (5)] and hence h increases; if $\Delta\theta$ increases faster than F_θ, w_e and hence h decreases. A perturbation in h implies a change in $\Delta\theta$, and eventually a new equilibrium is reached, in which w_e is back to its original value before the perturbation, that is, equal to w_{FT} [Eq. (3)]. Depending on the strength of the surface coupling, h has either increased or decreased.

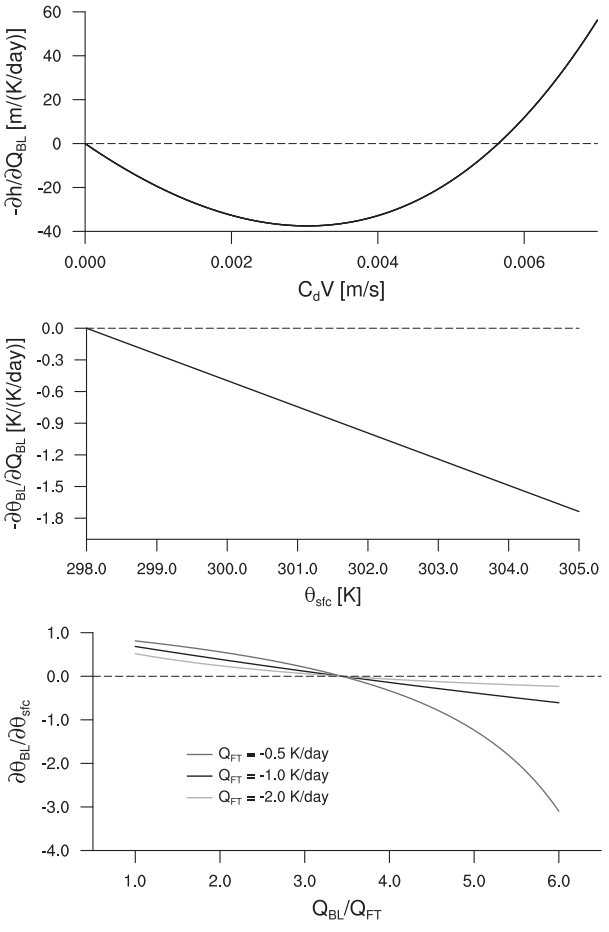

FIG. 5. (top) Change of the BL height with radiative BL cooling as a function of surface coupling. Negative values mean that the BL height decreases for stronger radiative BL cooling. (middle) Change of the BL potential temperature with radiative BL cooling as a function of surface potential temperature. (bottom) Change of the BL potential temperature with surface potential temperature as a function of the ratio of radiative cooling in the BL and in the FT.

2) Surface warming

Irrespective of the value of C_dV, the model also predicts some nonintuitive behavior in the response to surface warming. For the most part, the BL responds as one might expect to an increase in θ_{sfc}: h, $\Delta\theta$, and F_θ all increase (Fig. 4). This is expected as a positive perturbation in θ_{sfc} increases the temperature difference to the BL and therefore F_θ. Higher F_θ leads to more vigorous turbulence in the BL and an increase in h, which results

in an increase in $\Delta\theta$, all else equal. The BL temperature, however, shows a different, interesting behavior. For weak radiative BL cooling rates, θ_{BL} increases as expected with increasing θ_{sfc}. But for strong radiative BL cooling rates, this behavior reverses, which seems counterintuitive: θ_{BL} decreases with increasing θ_{sfc}; that is, a surface warming leads to a net cooling of the BL. In between, for a threshold of $Q_{BL,thres} = -3.4\,\mathrm{K\,day^{-1}}$, θ_{BL} is independent of θ_{sfc} (and of C_dV).

The reversal of the change of θ_{BL} with θ_{sfc} can be explained by analyzing θ_{BL} more closely. Solving Eqs. (1)–(6) for θ_{BL} gives

$$\theta_{BL} = \frac{\theta_0 + K_1\theta_{sfc}}{1+K_1}, \quad \text{with}$$
$$K_1 = \left[A - (A+1)\frac{Q_{FT}}{Q_{BL}}\right]\frac{C_dV}{w_{FT}}. \tag{8}$$

Differentiating Eq. (8) with respect to Q_{BL} shows that $\partial\theta_{BL}/\partial Q_{BL}$ is linearly dependent on θ_{sfc} with more negative values for higher θ_{sfc}; that is, θ_{BL} decreases faster than Q_{BL} for higher θ_{sfc} (Fig. 5, middle).

Differentiating Eq. (8) with respect to θ_{sfc} gives

$$\frac{\partial\theta_{BL}}{\partial\theta_{sfc}} = \frac{K_1}{1+K_1}. \tag{9}$$

It can be seen that $\partial\theta_{BL}/\partial\theta_{sfc} = 0$ for $K_1 = 0$, that is, if $Q_{BL}/Q_{FT} = (A+1)/A = 3.4$. Inserting $K_1 = 0$ in Eq. (8) shows that $\theta_{BL} = \theta_0$ and that θ_{BL} becomes independent of θ_{sfc} (and C_dV) in this situation. For $Q_{BL}/Q_{FT} < (A+1)/A$, θ_{BL} increases with θ_{sfc}, and, for $Q_{BL}/Q_{FT} > (A+1)/A$, θ_{BL} decreases with θ_{sfc} (Fig. 5, bottom). While the zero crossing is independent of all parameters except A, the magnitude of the change of θ_{BL} with θ_{sfc} depends on Q_{FT} and Q_{BL}, and absolute values are largest for weak radiative FT cooling.

Physically, this phenomenon can be explained by combining the budget equation for θ_{BL} [Eq. (1)] and the closure equation for the entrainment [Eq. (5)], which shows that entrainment heating of the BL, $w_e\Delta\theta/h$, is a fixed ratio of the negative value of the radiative BL cooling rate:

$$\frac{w_e\Delta\theta}{h} = \frac{A}{A+1}(-Q_{BL}) \approx 30\%(-Q_{BL}). \tag{10}$$

Therefore, for fixed Q_{BL} and fixed $Q_{FT}/\Gamma = w_e$, the ratio $\Delta\theta/h$ has to be the same in different equilibrium states. If θ_{sfc} is increased, F_θ increases as a result of a larger difference between θ_{BL} and θ_{sfc}. Increasing F_θ leads to more vigorous convective plumes and turbulence, thus h increases. For a fixed θ_{BL}, an increase in h means that $\Delta\theta$ increases (Fig. 6). To keep the ratio $\Delta\theta/h$ constant as implied by Eq. (10), $\Delta\theta$ has to increase exactly proportional to h. This is only the case if $\theta_{BL} = \theta_0$ [Eq. (4), Fig. 6b]. If $\theta_{BL} \neq \theta_0$, θ_{BL} has to adjust so that $\Delta\theta$ changes proportionally to h. For $\theta_{BL} > \theta_0$, $\Delta\theta$ increases overproportionately due to an increase in h. To compensate for this overproportional change, θ_{BL} needs to increase (Fig. 6a). Vice versa, for $\theta_{BL} < \theta_0$, $\Delta\theta$ increases underproportionately due to an increase in h. To compensate for this underproportional change, θ_{BL} needs to decrease (Fig. 6c).

To keep w_e constant in our idealized configuration, $\Delta\theta$ has to increase proportionally to h, for a given Q_{BL}. In nature, however, a decrease of θ_{BL} with increasing θ_{sfc} might be difficult to observe because other effects ranging from humidity gradients to a nonlinear profile of free-tropospheric temperature gradient may obscure such effects. Also, we expect that the radiative cooling rate of the BL will be less strong for increasing θ_{sfc}, which leads to an increase in θ_{BL}. Such a radiative feedback could overcompensate the decrease in θ_{BL} described before.

3) TEMPERATURE REGIMES

Further analyzing Eq. (8), three temperature regimes can be distinguished depending on the radiative cooling in the BL and in the FT (Fig. 7). Because radiation is not allowed to directly drive entrainment in the bulk model, a positive surface flux is required for an equilibrium, nonzero BL height; that is, $\theta_{BL} < \theta_{sfc}$. From Eq. (8), it can be seen that if $\theta_{sfc} = \theta_0$, the solution is unphysical because it directly follows that $\theta_{BL} = \theta_{sfc}$ and therefore $F_\theta = 0$. Provided that $\theta_{sfc} \neq \theta_0$, we can identify three regimes. Regime I and regime II are separated by the limiting case of $\theta_{BL} = \theta_0$, which requires

$$Q_{BL} = \frac{1+A}{A}Q_{FT} \tag{11}$$

and has been discussed earlier in section 2b(2). In regime I, $\theta_{BL} > \theta_0$, and the BL warms when θ_{sfc} increases. In regime II, $\theta_{BL} < \theta_0$, and the BL cools when θ_{sfc} increases. All the combination of parameters discussed earlier and in section 3 are situated within regime I and regime II.

There is, however, a third regime, which is separated from regime II by the limiting case of $\theta_{BL} \to 0\,\mathrm{K}$. Then the numerator of Eq. (8) has to go to zero, which gives

$$Q_{BL} = \frac{(1+A)C_dV\Gamma Q_{FT}\theta_{sfc}}{AC_dV\Gamma\theta_{sfc} + Q_{FT}\theta_0} \tag{12}$$

For $\theta_{sfc} \to \theta_0$, this is the limiting case between a regime that has physical solutions only if $\theta_{sfc} < \theta_0$ (regime III in Fig. 7) and a regime that has physical solutions only if $\theta_{sfc} > \theta_0$ (regime I and II). Regime III cannot be

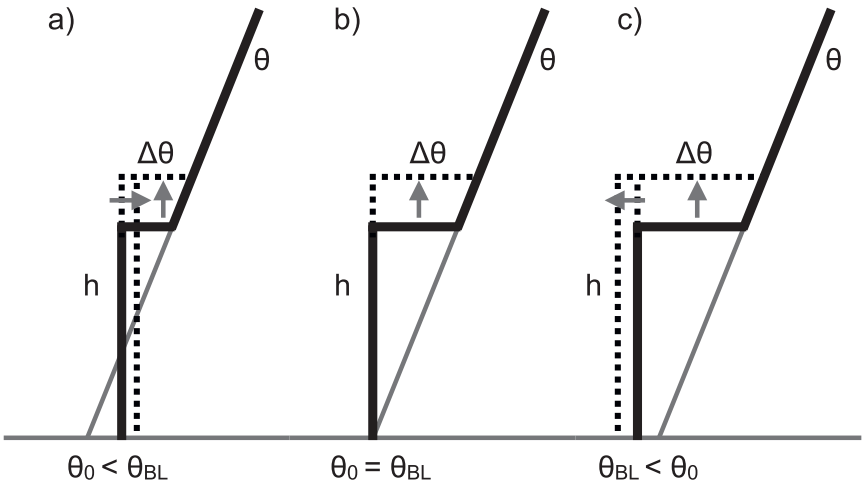

FIG. 6. Surface warming can either lead to a net warming or a net cooling of the BL depending on the prescribed radiative cooling rates in the bulk model: an increase in θ_{sfc}, all else being equal, leads to an initial increase in h and $\Delta\theta$. Because the ratio $\Delta\theta/h$ has to be kept constant, θ_{BL} needs to adjust. (a) θ_{BL} increases for $\theta_0 < \theta_{BL}$, (b) θ_{BL} is independent of θ_{sfc} for $\theta_0 = \theta_{BL}$, or (c) θ_{BL} decreases for $\theta_{BL} < \theta_0$. See text for more detailed explanation.

reached for strong radiative cooling in the FT with $-Q_{FT} > AC_dV\Gamma\theta_{sfc}/\theta_0$ (where $AC_dV\Gamma = 0.9\,\mathrm{K\,day^{-1}}$ for the values in Table 1), because the denominator of Eq. (12) needs to be positive for a positive θ_{BL}. For strong radiative FT cooling, the solution of the system becomes unphysical if $\theta_{sfc} < \theta_0$. Although regime III has physical solutions for $\theta_{sfc} < \theta_0$ and weak radiative FT cooling, we do not discuss these solutions further in this study because we are primarily interested in situations with moderate to strong FT subsidence (like in Fig. 1).

Physically, the limit of weak radiative FT cooling in regime III can be explained by the required balance between FT subsidence and the entrainment velocity at the inversion: According to the weak temperature gradient assumption [Eq. (2)], strong radiative FT cooling leads to strong subsidence. This subsidence is balanced by w_e [Eq. (3)], which is proportional to $F_\theta/\Delta\theta$ [Eq. (5)]. Therefore, strong entrainment can only be achieved if F_θ is large and if $\Delta\theta$ is small. Both conditions cannot be fulfilled at the same time if $\theta_{sfc} < \theta_0$ because large F_θ requires that θ_{BL} is substantially smaller than θ_{sfc} [Eq. (6)], but small $\Delta\theta$ requires that θ_{BL} is close to θ_0 [Eq. (4)]. Because h is also connected to $\Delta\theta$ [Eq. (4)], the BL collapses for strong radiative FT cooling if it cannot be balanced by strong entrainment, i.e., if $\theta_{sfc} < \theta_0$.

c. Nondimensional formulation

Besides C_dV, θ_{sfc}, and Q_{BL}, whose effects on the system are discussed in detail above, the properties of the FT can also change the state of the BL and its response to increasing radiative BL cooling. This dependence on FT properties can be easily embedded in the previous analysis with the help of dimensional analysis. As we show next, the dimensional analysis provides a complete representation of the system.

From Eqs. (2) and (3), we note that $w_{FT} = -w_e = Q_{BL}/\Gamma$. Rewriting Eqs. (1), (4), (5), and (6) in terms of temperature anomalies gives the following:

$$hQ_{BL} + (1+A)F_\theta = 0, \tag{13}$$

$$\theta_{BL} - \theta_0 = \Gamma h - \Delta\theta, \tag{14}$$

$$\Delta\theta = -\frac{AF_\theta}{w_{FT}}, \quad \text{and} \tag{15}$$

$$F_\theta = C_dV[(\theta_{sfc} - \theta_0) - (\theta_{BL} - \theta_0)]. \tag{16}$$

Given w_{FT}, Q_{BL}, $\theta_{sfc} - \theta_0$, A, C_dV, and Γ, these equations can be solved for h, $\theta_{BL} - \theta_0$, $\Delta\theta$, and F_θ. With this

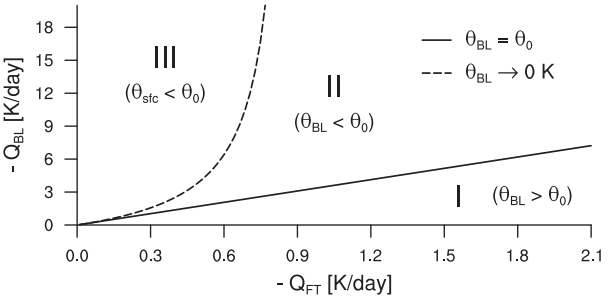

FIG. 7. In the parameter space of Q_{FT} and Q_{BL}, three temperature regimes are identified. In regimes I and II, $\theta_{sfc} > 0$. See text for further explanation.

formulation, we have three dimensions left: length, time, and temperature. We choose three reference parameters, w_{FT}, $\theta_{sfc} - \theta_0$, and Γ, to formulate characteristic scales for velocity, w_{FT}, temperature, $\theta_{sfc} - \theta_0$, and length, $L_0 = (\theta_{sfc} - \theta_0)/\Gamma$.

Now, we can rearrange Eqs. (13)–(16) and obtain the four normalized variables we are looking for:

$$\frac{h}{L_0} = \frac{\hat{V}}{(1-\hat{V})\hat{Q} + \hat{V}}, \tag{17}$$

$$\frac{\theta_{BL} - \theta_0}{\theta_{sfc} - \theta_0} = \frac{h}{L_0}(1-\hat{Q}), \tag{18}$$

$$\frac{\Delta\theta}{\theta_{sfc} - \theta_0} = \frac{h}{L_0}\hat{Q}, \quad \text{and} \tag{19}$$

$$\frac{F_\theta}{-w_{FT}(\theta_{sfc} - \theta_0)} = \frac{h}{L_0}\frac{\hat{Q}}{A} \tag{20}$$

as functions of only three parameters:

$$\hat{Q} = \frac{A}{1+A}\frac{Q_{BL}}{Q_{FT}}, \quad \hat{V} = A\frac{C_d V}{-w_{FT}}, \quad \text{and} \quad A. \tag{21}$$

The principle behavior of the bulk model can therefore be explored by varying only these three parameters. The last parameter, A, is strictly not an external parameter, but rather determined by the flow, which we fix on the basis of LES, where it is found to be constant (within an uncertainty because of model resolution). A change in $\hat{Q}$ can be interpreted in analog to a change in Q_{BL} and a change in $\hat{V}$ in analog to a change in $C_d V$. The condition $\hat{V} = 1$ distinguishes the velocity regimes discussed in section 2b(1): for $\hat{V} < 1$, the BL height decreases with a stronger radiative BL cooling, whereas it increases for $\hat{V} > 1$. The condition $\hat{Q} = 1$ distinguishes the temperature regimes discussed in sections 2b(2) and 2b(3): for $\hat{Q} < 1$, the BL temperature increases with a higher surface temperature, whereas it decreases for $\hat{Q} > 1$. Therefore, the principle behavior of the model equations for any set of parameters, including the FT parameters, can be derived from the results obtained by varying Q_{BL}, θ_{sfc}, and $C_d V$. We limit the discussion to these parameters also in the following section 3.

3. Circulation induced by low-level radiative cooling

Having found good agreement between the bulk model and the LES for horizontally homogeneous radiative cooling in section 2, we are now interested in how horizontally heterogeneous radiative cooling in the BL can drive a shallow larger-scale circulation. This circulation will then not be driven by surface temperature differences, but by differences in radiative cooling, for instance, associated with differences in the water vapor path above the BL. To do so, we use the case of vertically homogeneous radiative cooling (i.e., $Q_{BL} = Q_{FT} = -1\,\mathrm{K\,day^{-1}}$) as a reference in one region and increase the radiative BL cooling in a neighboring region. First, we discuss how to calculate the flow in the absence of feedbacks between the regions. This can be thought of as the strength of the flow that is associated with the pressure gradients that would arise from the thermodynamic differences in the two regions. In a second step, we allow for a shallow return flow and the feedback of the flow on the BL properties.

a. Flow speed

Increasing radiative cooling rates in the BL change the equilibrium temperature profile for homogeneous radiative cooling (Fig. 3) and hence the pressure profile. Integrating the hydrostatic equation over height gives the barometric formula, which is applied stepwise for height ranges with a linear temperature profile to calculate the pressure profile. Assuming that the pressure at a fixed height above the BL is the same in both regions and unaffected by what happens below it, a pressure deviation compared to the case with vertically homogeneous radiative cooling is calculated. This pressure deviation $\delta p'$ increases toward the surface, where it reaches its maximum, and also increases with increasing radiative BL cooling (Fig. 8a) because colder air is denser and heavier. Near the BL top, negative values of $\delta p'$ occur as a result of the change of the BL height with radiative BL cooling, that is, because the FT air is warmer and therefore lighter than BL air at the same height. Both the shape and the magnitude of the profiles of $\delta p'$ computed with the bulk model agree well with LES. Also, the profile of $\delta p'$ resembles well the shape of the horizontal flow speed between dry and moist patches found in simulations of organized convection (Fig. 1, middle).

To calculate the flow that arises from $\delta p'$, which is caused by the difference in radiative BL cooling as described above, we first formulate a momentum equation that is valid for the sum of the background flow V and the secondary circulation caused by the difference in radiative BL cooling. The simplified momentum equation neglects the Coriolis effect and assumes an equilibrium between the acceleration due to drag a_d and the acceleration due to a pressure gradient

$$a_d = -\rho^{-1}\frac{\partial p}{\partial x}, \tag{22}$$

where ρ is the air density, which varies little in the BL. Because we consider a horizontal area with the

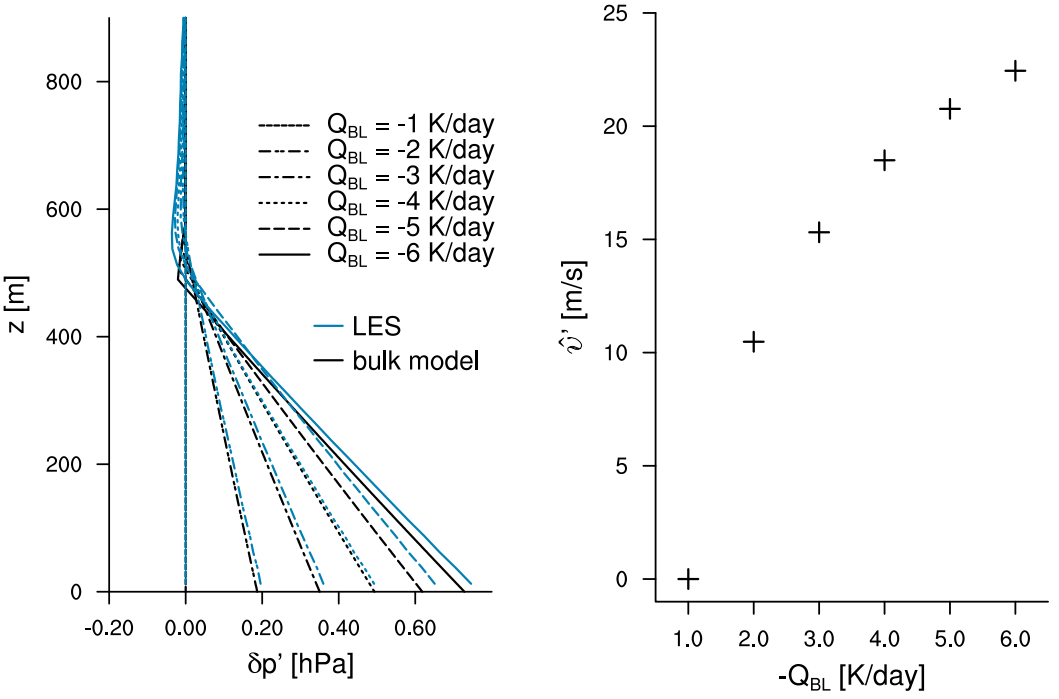

FIG. 8. (left) Profiles of pressure deviation from the case with vertically homogeneous radiative cooling for the LES (blue) and the bulk model (black). (right) Initial flow velocity of the secondary circulation due to $\delta\hat{p}'$ as a function of the radiative BL cooling according to Eq. (25).

boundaries at the cold column and at the warm column, the horizontal velocity difference between these boundaries is zero, and the advection term drops out. Integrating Eq. (22) from the surface to the BL height, neglecting drag at the inversion, and assuming a linear decrease of the horizontal pressure gradient with height gives

$$C_d\hat{v}^2 = \rho^{-1}\frac{h}{X_p}\delta\hat{p}, \tag{23}$$

where $X_p = 20\,\text{km}$ is the horizontal extent of the pressure gradient (cf. to Fig. 1, left), which is a prescribed parameter (Table 1). Furthermore, $\hat{v}$ and $\delta\hat{p}$ are the BL mean flow velocity and the BL mean pressure deviation, respectively. They can be written as the sum of their background contribution (V and P) and the deviation due to a secondary circulation ($\hat{v}'$ and $\hat{p}'$), that is, $\hat{v} = V + \hat{v}'$ and $\hat{p} = P + \hat{p}'$. We consider the case where the background flow and the secondary circulation are directed in the same direction ($\hat{v} > 0$). Subtracting the background state, $C_d V^2 = \rho^{-1}(h/X_p)\delta P$, from Eq. (23) gives

$$C_d(\hat{v}'^2 + 2V\hat{v}') = \rho^{-1}\frac{h}{X_p}\delta\hat{p}', \tag{24}$$

where $\delta\hat{p}' = 1/2\delta p'^2_{\text{sfc}}/(\delta p'_{\text{sfc}} - \delta p'_h)$. Here, we assume that a negative $\delta\hat{p}'$ has no effect on the BL flow but is implicitly considered later in a return flow. The factor $\delta p'_{\text{sfc}}/(\delta p'_{\text{sfc}} - \delta p'_h)$ ensures that only the positive pressure perturbations in the BL are taken into account. In Eq. (24), $2V\hat{v}'$ is a cross term in the drag formulation that is caused by the interaction between the background flow and the secondary circulation. Solving Eq. (24) for $\hat{v}'$ finally leads to

$$\hat{v}' = -V + \sqrt{V^2 + \frac{1}{C_d\rho}\frac{h}{X_p}\delta\hat{p}'}. \tag{25}$$

It can be seen that, for a given pressure deviation, $\hat{v}'$ is always smaller if $V > 0$ than without a background flow because friction is more effective at higher flow speed.

Like the pressure deviation, $\hat{v}'$ increases with increasing radiative BL cooling (Fig. 8, right). Hence, the BL divergence also increases with increasing radiative BL cooling. Because no feedback of the flow on the BL structure is included yet, $\hat{v}'$ represents an initial flow speed for the case of two separate regions with different radiative BL cooling each in equilibrium, which are then abruptly allowed to interact. As expected, such an initial $\hat{v}'$is considerably higher than the flow speed of a shallow circulation between dry and moist patches found in simulations of organized convection (Fig. 1, middle; Hohenegger and Stevens 2016). Also, hydrodynamic effects on the pressure gradient and the detailed flow

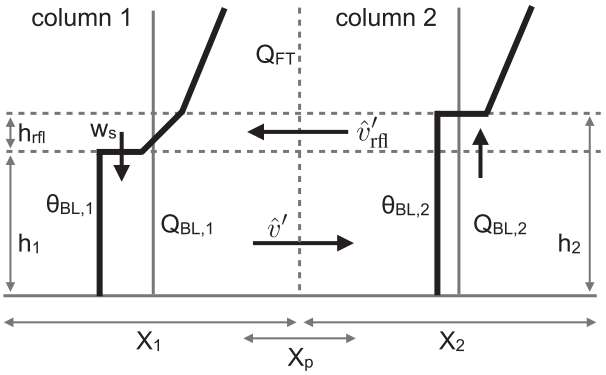

FIG. 9. Sketch of the two-column model with radiative BL cooling Q_{BL} being stronger in column 1 than in column 2 ($|Q_{BL,1}| > |Q_{BL,2}| \geq |Q_{FT}|$).

dynamics are not taken into account. This is justified here because we are interested in the first-order response of the system to the thermal contrast set by radiative cooling. Nevertheless, the subtleties in the pressure adjustment merit further investigation, for example, by formulating a continuous (x resolved) form of the momentum equation or by using LES.

b. *Two-column model including circulation feedback*

To allow for feedbacks between two regions with different radiative BL cooling rates, we formulate a two-column model, where the radiative BL cooling is stronger in column 1 than in column 2 (Fig. 9). With the prescribed parameters in Table 1, this leads to a shallower BL in column 1 and a near-surface flow from column 1 to column 2, which advects colder air into column 2. We assume that a return flow $\hat{v}'_{rfl}$, which is needed to conserve mass in the domain, is located below the inversion in column 2 but above the inversion in column 1. This assumption is motivated by RCE simulations, which show that the return-flow layer is indeed shallow and restricted to the height of the BL (Fig. 1, middle). The vertical part of the induced circulation lowers the BL height of column 1 while the BL height of column 2 remains unaffected (although h_2 can still change according to a change in $\theta_{BL,2}$).

The equations of the two-column model are similar to those for the homogeneous case [Eqs. (1)–(6)] but include advective terms and additional equations for the return-flow layer. Also, we do not assume equilibrium anymore but analyze the response of the system—the circulation feedback—until a new equilibrium is reached. As initial conditions for each column, we use the equilibrium solution for homogeneous radiative cooling (section 2).

The modified equations for column 1 are as follows:

$$\frac{\partial \theta_{BL,1}}{\partial t} = Q_{BL,1} + \frac{A+1}{h_1} F_{\theta,1}, \tag{26}$$

$$\frac{\partial h_1}{\partial t} = w_{FT} + w_{e,1} + w_s = \frac{Q_{FT}}{\Gamma} + \frac{A F_{\theta,1}}{\Delta\theta_1} - \hat{v}' \frac{h_1}{X_1}, \tag{27}$$

$$F_{\theta,1} = C_d \left(V + \frac{1}{2}\hat{v}' \right) (\theta_{sfc,1} - \theta_{BL,1}), \quad \text{and} \tag{28}$$

$$\Delta\theta_1 = \theta_{rfl} - \Gamma_{rfl} \frac{h_2 - h_1}{2} - \theta_{BL,1}. \tag{29}$$

For column 2:

$$\frac{\partial \theta_{BL,2}}{\partial t} = Q_{BL,2} + \frac{A+1}{h_2} F_{\theta,2} + \hat{v}' \frac{\theta_{BL,1} - \theta_{BL,2}}{X_2} \frac{h_1}{h_2}, \tag{30}$$

$$\frac{\partial h_2}{\partial t} = w_{FT} + w_{e,2} = \frac{Q_{FT}}{\Gamma} + \frac{A F_{\theta,2}}{\Delta\theta_2}, \tag{31}$$

$$F_{\theta,2} = C_d \left(V + \frac{1}{2}\hat{v}' \right) (\theta_{sfc,2} - \theta_{BL,2}), \quad \text{and} \tag{32}$$

$$\Delta\theta_2 = \theta_0 + \Gamma h_2 - \theta_{BL,2}. \tag{33}$$

For the return-flow layer of column 1:

$$\frac{\partial \theta_{rfl}}{\partial t} = Q_{FT} - \left(w_{FT} + \frac{1}{2} w_s \right) \Gamma_{rfl} + \hat{v}'_{rfl} \frac{\theta_{BL,2} - \theta_{rfl}}{X_1}, \tag{34}$$

$$\hat{v}'_{rfl} = \hat{v}' \frac{h_1}{h_2 - h_1}, \quad \text{and} \tag{35}$$

$$\Gamma_{rfl} = \frac{\theta_0 + \Gamma h_2 - \theta_{rfl}}{0.5(h_2 - h_1)}, \tag{36}$$

where the subscripts 1, 2, and rfl indicate that a variable is associated with column 1, column 2, or the return-flow layer, respectively. The horizontal sizes of the columns, X_1 and X_2, are assumed to be equal ($X_1 = X_2 = 100$ km, Table 1) and represent the size of a nonconvective area (cf. to Fig. 1, left). Moreover, Q_{FT}, θ_0, Γ, and hence also w_{FT}, are assumed to be the same in column 1 and column 2. The temperature in the return-flow layer of column 1 is assumed to increase linearly with height with a gradient of Γ_{rfl} and is assumed to be equal to the FT temperature at h_2. The quantity θ_{rfl} represents the mean temperature of the return-flow layer. The vertical part of the induced circulation reaches its maximum value, w_s, at h_1. We assume that w_s decreases linearly to zero at h_2; that is, that $\hat{v}'_{rfl}$ is constant with height.

Physically, w_s lowers the BL height of column 1 [Eq. (27)] and warms the return-flow layer by subsidence warming in addition to w_{FT} [second term on the right-hand side of Eq. (34)]. Advection of heat is included in the prognostic equations for potential temperature in

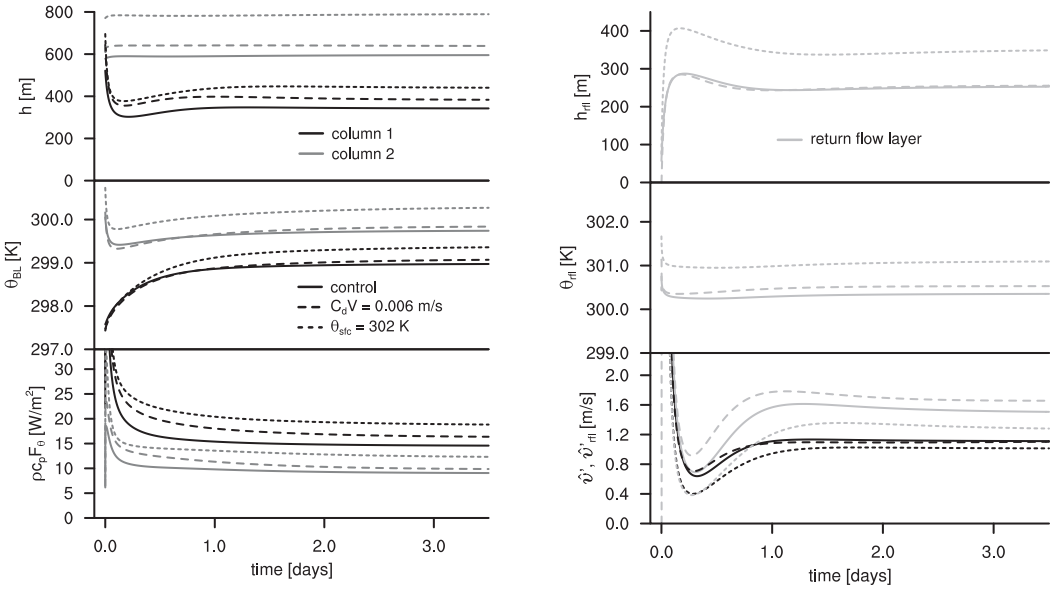

FIG. 10. Transient response of the two-column model to heterogeneous radiative cooling. Simulation parameters are the same as in Fig. 4, and initial conditions are the equilibrium simulations with homogeneous radiative cooling applying a stronger radiative BL cooling in column 1 ($Q_{BL,1} = -4\,\mathrm{K\,day^{-1}}$) than in column 2 ($Q_{BL,2} = -1\,\mathrm{K\,day^{-1}}$). Line colors indicate the column or the return-flow layer; line patterns indicate the case setup.

column 2 due to the BL flow [last term on the right-hand side of Eq. (30)] and in the return-flow layer due to the return flow [last term on the right-hand side of Eq. (34)]. In Eq. (29), which defines the temperature jump at the inversion, $\theta_{rfl} - \Gamma_{rfl}(h_2 - h_1)/2$ is the temperature just above the inversion, that is, at the bottom of the return-flow layer.

c. *Transient response*

We first discuss results for a stronger radiative BL cooling in column 1 of $Q_{BL,1} = -4\,\mathrm{K\,day^{-1}}$ and a weaker radiative BL cooling in column 2 of $Q_{BL,2} = -1\,\mathrm{K\,day^{-1}}$ (Fig. 10). The surface temperature is equal in both columns. For the control case with $C_dV = 0.005\,\mathrm{m\,s^{-1}}$ and $\theta_{sfc} = 301\,\mathrm{K}$, the BL height of column 1, h_1, decreases as expected because the circulation pushes the inversion height down by an additional subsidence term w_s. The shallowing BL of column 1 leads to a warming compared to the uncoupled case; that is, $\theta_{BL,1}$ increases, while the surface flux $F_{u,1}$ decreases. In column 2, the BL temperature, $\theta_{BL,2}$, decreases as expected because relatively cold air is advected from column 1 into column 2. Also, $F_{\theta,2}$ decreases because $\hat{v}'$decreases. The increase in $\theta_{BL,1}$ and the decrease of the temperature of the return-flow layer in column 1, θ_{rfl}, due to advection of air from the BL of column 2, lead to a decrease in the temperature jump at the inversion of column 1, $\Delta\theta_1$. The height of the return-flow layer, $h_{rfl} = h_2 - h_1$, is initially about 50 m and increases in the following by about 200 m, which is the amount that h_1 decreases.

Except for $\theta_{BL,2}$ and $F_{\theta,2}$, other variables in column 2 do not change much. The approaching BL temperatures of columns 1 and 2 (the cooler column 1 is warming while the warmer column 2 is cooling) lead to a decrease in pressure difference between the columns and therefore to a decrease in the horizontal flow $\hat{v}'$ to about $1\,\mathrm{m\,s^{-1}}$. The flow in the inversion $\hat{v}'_{rfl}$ also decreases strongly as a result of both the decrease in $\hat{v}'$ and the increase in h_{rfl}. Despite the decrease in wind speed, a circulation is maintained, and a new equilibrium is reached.

During transient adjustment, before the new equilibrium is reached, h_1 and $\hat{v}'$ depict a clear minimum. It would be interesting to see whether such a minimum in particular for the BL height also exists if cloud processes are included in the bulk model because this might have the potential to evaporate a stratocumulus deck. In the bulk model, the change of the BL height with time in column 1 is given by the sum of three vertical velocities: the FT subsidence velocity, the entrainment velocity, and the vertical part of the induced circulation [Eq. (27)]. The FT subsidence velocity is directed downward and constant in time because Q_{FT} and Γ are fixed. The entrainment velocity is directed upward but changes more slowly in time than the induced circulation, whose vertical component in column 1 is directed downward. Therefore, h_1 decreases initially due to a dominance of

the induced circulation, which introduces a faster time scale, but increases later due to a dominance of the entrainment velocity. After about 2 days, a new equilibrium is reached, in which the three vertical velocities in column 1 balance.

If the surface coupling is stronger ($C_dV = 0.006\,\mathrm{m\,s^{-1}}$), the BL height increases with radiative BL cooling, that is, $h_1 > h_2$ initially [section 2b(1)]. If $h_1 > h_2$ with $p_1 > p_2$, h_{rfl} is negative, and we assume that there is no return flow above h_2. However, a BL flow still develops, and, to satisfy mass conservation, the air that is advected by $\hat{v}'$ from column 1 to column 2 leads to an increase in h_2 and a decrease in h_1 until $h_1 < h_2$. The process happens very quickly (within a few minutes), and the subsequent development of the system is similar to the case of weak surface coupling described before. In particular, the flow in the BL, $\hat{v}'$, is very similar in magnitude to the control case with weaker surface coupling.

For a higher surface temperature ($\theta_{\mathrm{sfc}} = 302\,\mathrm{K}$), the temperature in both columns changes more strongly than in the control case. Also, h_{rfl} is larger and h_1 decreases more strongly in absolute terms. In relative terms, h_1 is about twice as large as h_{rfl}, which is similar to the control case. The flow in the BL $\hat{v}'$ is only slightly weaker but overall again similar in magnitude to the control case with lower surface temperature. This suggests a strong negative feedback associated with the circulation, which decreases $\hat{v}'$ to a similar magnitude and makes the two-column model less sensitive to changes in the parameters than in the homogeneous setup in section 2.

d. Equilibrium solution

Focusing on the equilibrium solution of the two-column model, we find that h_1 decreases with larger differences in radiative BL cooling between the columns and with lower surface temperature (Fig. 11, left). This decrease is qualitatively similar to the homogeneous setup but stronger in magnitude (cf. to Fig. 4). Also, $\theta_{\mathrm{BL},1}$ decreases with larger difference in radiative BL cooling and with lower surface temperature but less than in the homogeneous case. In particular, $\theta_{\mathrm{BL},1}$ decreases with decreasing surface temperature for the full range of applied $Q_{\mathrm{BL},1}$ (Fig. 11, left)—contrary to the homogeneous case—because $w_{e,1}$ does not need to be constant for changing surface temperature [Eq. (27)]. In column 2, where $Q_{\mathrm{BL},2}$ is constant, h_2 does not change with increasing difference in radiative BL cooling, but $\theta_{\mathrm{BL},2}$ decreases slightly because of advection of colder air from column 1.

The circulation in the BL is generally weak ($\hat{v}' \approx 1\,\mathrm{m\,s^{-1}}$) for the heterogenous setup and decreases for radiative BL cooling differences smaller than $1\,\mathrm{K\,day^{-1}}$, when the BL heights and the BL temperatures in column 1 and column 2 are close to each other (Fig. 11, left). In the return-flow layer, $\hat{v}'_{\mathrm{rfl}}$ depends strongly on h_{rfl} and increases when h_1 approaches h_2 for small radiative BL cooling differences. For radiative BL cooling differences larger than $1\,\mathrm{K\,day^{-1}}$, the BL flow is surprisingly little affected by the magnitude of the radiative BL cooling difference or θ_{sfc} (Fig. 11, left).

To compare the effectiveness of heterogeneous radiative BL cooling and heterogeneous surface temperatures in causing a shallow circulation (e.g., Lindzen and Nigam 1987), we analyze the equilibrium solution of the two-column model for the same radiative cooling rates prescribed in both columns but a higher surface temperature prescribed in column 2 than in column 1 ($\theta_{\mathrm{sfc},1} = 301\,\mathrm{K} < \theta_{\mathrm{sfc},2}$). The surface pressure in column 1 and column 2 is governed by two effects: for a large BL height, the surface pressure will be high because BL air is colder and hence denser than FT air; for a high BL temperature, the surface pressure will be low because warm BL air is less dense than colder BL air. Because for increasing surface temperature the BL temperature increases or decreases depending on the strength of the radiative BL cooling [section 2b(2)], either of the two effects can dominate. For strong radiative BL cooling, the increase in surface pressure due to the increase in BL height with surface temperature dominates over the decrease in surface pressure due to the increase in BL temperature so that column 2 has a higher surface pressure. Therefore, the induced flow is directed from the column with higher θ_{sfc} to the column with lower θ_{sfc}, opposite of what we anticipate from a land–sea breeze. Because we do not expect decreasing θ_{BL} with increasing θ_{sfc} to show up in nature [section 2b(2)], we do not discuss the case of strong radiative BL cooling in terms of the circulation feedback here. Note, however, that a flow from areas of high θ_{sfc} to areas of low θ_{sfc} has occasionally been observed in RCE studies of organizing convection (Hohenegger and Stevens 2016). We suspect that, in these cases, other effects, such as differences in radiative cooling, humidity, and evaporative cooling have dominated the circulation's direction and strength.

For weak radiative BL cooling rates ($Q_{\mathrm{BL}} > -2\,\mathrm{K\,day^{-1}}$), the BL temperature effect dominates, and $p'_{\mathrm{sfc},1}$, which is associated with low $\theta_{\mathrm{sfc},1}$, is larger than $p'_{\mathrm{sfc},2}$. Hence a BL flow $\hat{v}'$ from column 1 to column 2 develops (Fig. 11, right). Applying larger differences in surface temperature, h_{rfl} and the difference between $\theta_{\mathrm{BL},1}$ and $\theta_{\mathrm{BL},2}$ increase. The strength of the BL flow $\hat{v}'$ increases slowly with increasing $\theta_{\mathrm{BL},2}$ but also depends on the strength of the radiative BL cooling. A difference in θ_{sfc} of a few kelvins causes a BL flow of approximately half the

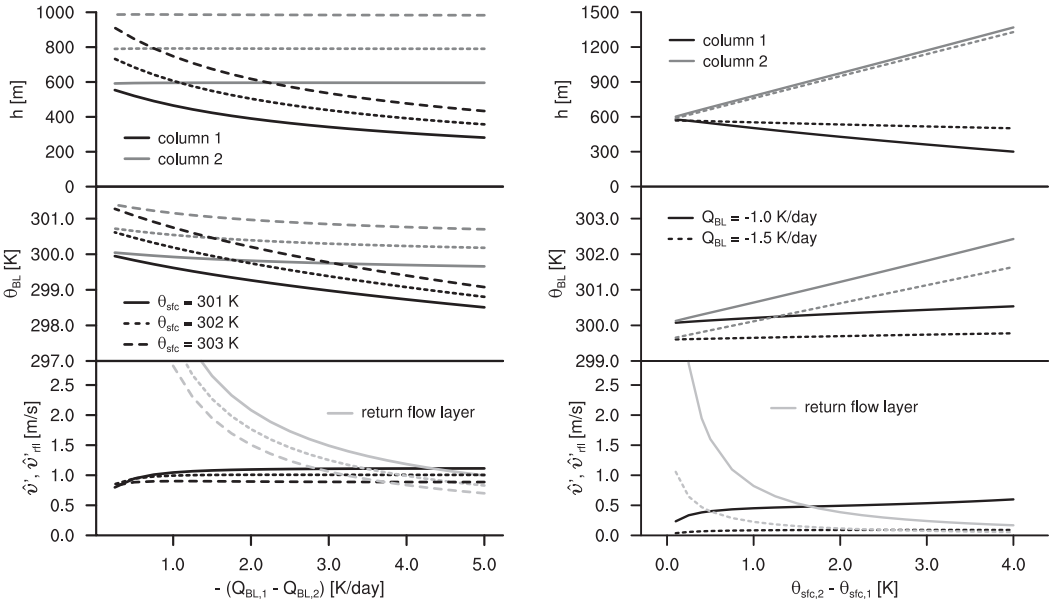

FIG. 11. (left) Equilibrium solution of the two-column model h, u_{BL}, and $\hat{v}'_{rfl}$ as a function of the difference in radiative BL cooling between the columns. In column 1, $Q_{BL,1}$ is fixed between -1 and -6 K day^{-1}. In column 2, $Q_{BL,2} = -1$ K day^{-1} in all cases. Line patterns indicate the surface temperature, which is the same in both columns. (right) As in the left panel, but as a function of the difference in surface temperature between the columns. In column 2, $\theta_{sfc,2}$ is fixed between 301.0 and 305.0 K. In column 1, $\theta_{sfc,1} = 301.0$ K in all cases. Line patterns indicate the radiative BL cooling, which is the same in both columns. In both panels, line colors indicate the column or the return-flow layer.

strength, as does a difference in Q_{BL} of a few kelvins per day. Hence, for a shallow circulation to develop, differences in radiative BL cooling can be as effective as differences in surface temperature.

4. Conclusions

We develop a conceptual model to analyze the link between low-level radiative cooling, surface forcing, boundary layer (BL) properties, and a shallow circulation, which has implications for determining the mechanisms for aggregation of convection and the formation of a shallow meridional circulation over tropical oceans. The conceptual model is representative for an equilibrium, dry, convective boundary layer and applies prescribed horizontally homogeneous low-level radiative cooling rates [Eqs. (1)–(6)]. It is found that, for a given free-tropospheric forcing, the principle behavior of the bulk model can be described by varying three external parameters: the radiative BL cooling, the surface temperature, and the strength of the surface coupling. Nondimensional analysis shows that this dependence can be reduced to two nondimensional parameters. Large-eddy simulations without moisture and with prescribed radiative cooling rates match the results of the bulk model very well, which gives us confidence that the formulation of the bulk model equations captures all processes important for the equilibrium state.

We find that, depending on the strength of the coupling to the surface, the BL height can decrease or increase in response to increasing homogeneous radiative BL cooling: for weak surface coupling the BL height decreases with increasing radiative BL cooling, while for strong surface coupling the BL height increases with increasing radiative BL cooling. This change in behavior is due to a dependence of the BL height on how fast the surface flux changes with BL temperature. Physically, a stronger radiative BL cooling decreases the BL temperature, which perturbs the entrainment rate both through an increase in surface flux and in inversion strength. Depending on whether the effect of the surface flux or the inversion strength dominates, the BL height increases or decreases, respectively.

Another counterintuitive finding revealed by the bulk model is that, for increasing surface temperature, the BL temperature decreases if the prescribed radiative BL cooling rates are strong. For weak radiative BL cooling rates, the BL temperature increases with increasing surface temperature, as expected. This behavior is caused by the formulation of the entrainment at the inversion, which implies that the ratio of the inversion strength to the BL height is constant for fixed

radiative BL cooling rates. A positive perturbation in surface temperature leads to an increase in BL height and an associated increase in inversion strength. This associated increase in inversion strength is proportional to the increase in BL height only if the ratio of the radiative BL cooling rate to the radiative free-tropospheric cooling equals $(A + 1)/A$, where A is the inversion entrainment efficiency. If the ratio deviates from this value, the BL temperature needs to adjust so that the inversion strength remains proportional to the BL height. For strong radiative BL cooling, this requires a decrease in BL temperature for increasing surface temperature.

Furthermore, we extend the bulk model to represent horizontally heterogeneous radiative BL cooling [Eqs. (26)–(36)]. As an initial response to heterogeneous radiative BL cooling, a pressure deviation develops between the area of weak radiative BL cooling and the area of strong radiative BL cooling. The shape and the magnitude of the pressure deviation profiles agree well with LES results. This pressure deviation then induces a circulation that resembles the shallow circulation found in simulations of organized moist convection.

To include the feedback of the induced circulation in the bulk model, we assume that the height of the return flow is limited by the BL height in the area with weak radiative BL cooling. The induced circulation leads to a new equilibrium, which is typically reached within 2 days. In this equilibrium, the BL height is reduced, and the BL temperature is increased in the area of strong radiative BL cooling compared to the uncoupled, homogeneous bulk model. Therefore, the pressure gradient between the two areas decreases, and the circulation strength weakens. Despite this weakening, a horizontal BL flow is maintained for all parameters tested when its feedback on the BL structure is included. For a difference in radiative BL cooling stronger than 1 K day^{-1}, the strength of the BL flow is about 1 m s^{-1} and only weakly dependent on stronger radiative BL cooling or increasing surface temperatures.

A shallow circulation caused by spatial differences in radiative BL cooling is found to be comparable in strength to a shallow circulation caused by spatial differences in surface temperature. This result implies that differences in radiative BL cooling should be considered in order to understand the mechanisms for convective aggregation and the formation of a shallow meridional circulation over tropical oceans. This is also in line with RCE simulations of organizing convection, where a circulation due to surface temperature differences can be found to be opposed to a circulation due to radiative cooling differences, and the competition between the two potentially leads to a delay in aggregation of convection or to the circulation switching sign with time (Hohenegger and Stevens 2016). Despite surface temperature gradients, spatial differences in radiative BL cooling should therefore also be considered as possible mechanisms for the formation of shallow circulations.

Acknowledgments. We thank James Ruppert, Tim Cronin, and two anonymous reviewers for helpful comments on the manuscript. Primary data and scripts used in the analysis and other supplementary information that may be useful in reproducing the author's work are archived by the Max Planck Institute for Meteorology and can be obtained by contacting publications@mpimet.mpg.de. This research was carried out as part of the Hans-Ertel Centre for Weather Research. This research network of universities, research institutes, and the Deutscher Wetterdienst is funded by the Federal Ministry of Transport and Digital Infrastructure (BMVI).

REFERENCES

Back, L. E., and C. S. Bretherton, 2009: On the relationship between SST gradients, boundary layer winds, and convergence over the tropical oceans. *J. Climate*, **22**, 4182–4196, doi:10.1175/2009JCLI2392.1.

Ball, F., 1960: Control of inversion height by surface heating. *Quart. J. Roy. Meteor. Soc.*, **86**, 483–494, doi:10.1002/qj.49708637005.

Beucler, T., and T. W. Cronin, 2016: Moisture-radiative cooling instability. *J. Adv. Model. Earth Syst.*, **8**, 1620–1640, doi:10.1002/2016MS000763.

Bretherton, C. S., P. N. Blossey, and M. Khairoutdinov, 2005: An energy-balance analysis of deep convective self-aggregation above uniform SST. *J. Atmos. Sci.*, **62**, 4273–4292, doi:10.1175/JAS3614.1.

Coppin, D., and S. Bony, 2015: Physical mechanisms controlling the initiation of convective self-aggregation in a general circulation model. *J. Adv. Model. Earth Syst.*, **7**, 2060–2078, doi:10.1002/2015MS000571.

Craig, G., and J. Mack, 2013: A coarsening model for self-organization of tropical convection. *J. Geophys. Res. Atmos.*, **118**, 8761–8769, doi:10.1002/jgrd.50674.

Deardorff, J. W., G. E. Willis, and D. K. Lilly, 1969: Laboratory investigation of non-steady penetrative convection. *J. Fluid Mech.*, **35**, 7–31, doi:10.1017/S0022112069000942.

——, ——, and ——, 1974: Comment on the paper by A. K. Betts "Non-precipitating cumulus convection and its parameterization." *Quart. J. Roy. Meteor. Soc.*, **100**, 122–123, doi:10.1002/qj.49710042311.

Emanuel, K., A. A. Wing, and E. M. Vincent, 2014: Radiative-convective instability. *J. Adv. Model. Earth Syst.*, **6**, 75–90, doi:10.1002/2013MS000270.

Fermepin, S., and S. Bony, 2014: Influence of low-cloud radiative effects on tropical circulation and precipitation. *J. Adv. Model. Earth Syst.*, **6**, 513–526, doi:10.1002/2013MS000288.

Garcia, J. R., and J. P. Mellado, 2014: The two-layer structure of the entrainment zone in the convective boundary layer. *J. Atmos. Sci.*, **71**, 1935–1955, doi:10.1175/JAS-D-13-0148.1.

Held, I. M., R. S. Hemler, and V. Ramaswamy, 1993: Radiative-convective equilibrium with explicit two-dimensional moist convection. *J. Atmos. Sci.*, **50**, 3909–3927, doi:10.1175/1520-0469(1993)050<3909:RCEWET>2.0.CO;2.

Hohenegger, C., and B. Stevens, 2016: Coupled radiative convective equilibrium simulations with explicit and parameterized convection. *J. Adv. Model. Earth Syst.*, **8**, 1468–1482, doi:10.1002/2016MS000666.

Holloway, C., and S. Woolnough, 2016: The sensitivity of convective aggregation to diabatic processes in idealized radiative-convective equilibrium simulations. *J. Adv. Model. Earth Syst.*, **8**, 166–195, doi:10.1002/2015MS000511.

Jeevanjee, N., and D. M. Romps, 2013: Convective self-aggregation, cold pools, and domain size. *Geophys. Res. Lett.*, **40**, 994–998, doi:10.1002/grl.50204.

Lindzen, R. S., and S. Nigam, 1987: On the role of sea surface temperature gradients in forcing low-level winds and convergence in the tropics. *J. Atmos. Sci.*, **44**, 2418–2436, doi:10.1175/1520-0469(1987)044<2418:OTROSS>2.0.CO;2.

Muller, C. J., and S. Bony, 2015: What favors convective aggregation and why? *Geophys. Res. Lett.*, **42**, 5626–5634, doi:10.1002/2015GL064260.

——, and I. M. Held, 2012: Detailed investigation of the self-aggregation of convection in cloud-resolving simulations. *J. Atmos. Sci.*, **69**, 2551–2565, doi:10.1175/JAS-D-11-0257.1.

Neelin, J. D., and I. M. Held, 1987: Modeling tropical convergence based on the moist static energy budget. *Mon. Wea. Rev.*, **115**, 3–12, doi:10.1175/1520-0493(1987)115<0003:MTCBOT>2.0.CO;2.

Neggers, R. A., J. D. Neelin, and B. Stevens, 2007: Impact mechanisms of shallow cumulus convection on tropical climate dynamics. *J. Climate*, **20**, 2623–2642, doi:10.1175/JCLI4079.1.

Nicholls, M. E., R. A. Pielke, and W. R. Cotton, 1991: Thermally forced gravity waves in an atmosphere at rest. *J. Atmos. Sci.*, **48**, 1869–1884, doi:10.1175/1520-0469(1991)048<1869:TFGWIA>2.0.CO;2.

Nilsson, J., and K. A. Emanuel, 1999: Equilibrium atmospheres of a two-column radiative-convective model. *Quart. J. Roy. Meteor. Soc.*, **125**, 2239–2264, doi:10.1002/qj.49712555814.

Nishant, N., S. Sherwood, and O. Geoffroy, 2016: Radiative driving of shallow return flows from the ITCZ. *J. Adv. Model. Earth Syst.*, **8**, 831–842, doi:10.1002/2015MS000606.

Nolan, D. S., C. Zhang, and S.-h. Chen, 2007: Dynamics of the shallow meridional circulation around intertropical convergence zones. *J. Atmos. Sci.*, **64**, 2262–2285, doi:10.1175/JAS3964.1.

Pierrehumbert, R. T., 1995: Thermostats, radiator fins, and the local runaway greenhouse. *J. Atmos. Sci.*, **52**, 1784–1806, doi:10.1175/1520-0469(1995)052<1784:TRFATL>2.0.CO;2.

Raymond, D. J., and X. Zeng, 2000: Instability and large-scale circulations in a two-column model of the tropical troposphere. *Quart. J. Roy. Meteor. Soc.*, **126**, 3117–3135, doi:10.1002/qj.49712657007.

Sobel, A. H., and C. S. Bretherton, 2000: Modeling tropical precipitation in a single column. *J. Climate*, **13**, 4378–4392, doi:10.1175/1520-0442(2000)013<4378:MTPIAS>2.0.CO;2.

——, and J. D. Neelin, 2006: The boundary layer contribution to intertropical convergence zones in the quasi-equilibrium tropical circulation model framework. *Theor. Comput. Fluid Dyn.*, **20**, 323–350, doi:10.1007/s00162-006-0033-y.

Stevens, B., 2006: Bulk boundary-layer concepts for simplified models of tropical dynamics. *Theor. Comput. Fluid Dyn.*, **20**, 279–304, doi:10.1007/s00162-006-0032-z.

——, 2007: On the growth of layers of non-precipitating cumulus convection. *J. Atmos. Sci.*, **64**, 2916–2931, doi:10.1175/JAS3983.1.

——, and Coauthors, 2005: Evaluation of large-eddy simulations via observations of nocturnal marine stratocumulus. *Mon. Wea. Rev.*, **133**, 1443–1462, doi:10.1175/MWR2930.1.

Tiedtke, M., W. Heckley, and J. Slingo, 1988: Tropical forecasting at ECMWF: The influence of physical parametrization on the mean structure of forecasts and analyses. *Quart. J. Roy. Meteor. Soc.*, **114**, 639–664, doi:10.1002/qj.49711448106.

Torn, R. D., and C. A. Davis, 2012: The influence of shallow convection on tropical cyclone track forecasts. *Mon. Wea. Rev.*, **140**, 2188–2197, doi:10.1175/MWR-D-11-00246.1.

Trenberth, K. E., D. P. Stepaniak, and J. M. Caron, 2000: The global monsoon as seen through the divergent atmospheric circulation. *J. Climate*, **13**, 3969–3993, doi:10.1175/1520-0442(2000)013<3969:TGMAST>2.0.CO;2.

van Heerwaarden, C., J. V.-G. de Arellano, A. Moene, and A. Holtslag, 2009: Interactions between dry-air entrainment, surface evaporation and convective boundary-layer development. *Quart. J. Roy. Meteor. Soc.*, **135**, 1277–1291, doi:10.1002/qj.431.

Wang, Y., S.-P. Xie, B. Wang, and H. Xu, 2005: Large-scale atmospheric forcing by southeast Pacific boundary layer clouds: A regional model study. *J. Climate*, **18**, 934–951, doi:10.1175/JCLI3302.1.

Wing, A. A., and K. A. Emanuel, 2013: Physical mechanisms controlling self-aggregation of convection in idealized numerical modeling simulations. *J. Adv. Model. Earth Syst.*, **6**, 59–74, doi:10.1002/2013MS000269.

Wu, Z., 2003: A shallow CISK, deep equilibrium mechanism for the interaction between large-scale convection and large-scale circulations in the tropics. *J. Atmos. Sci.*, **60**, 377–392, doi:10.1175/1520-0469(2003)060<0377:ASCDEM>2.0.CO;2.

——, D. S. Battisti, and E. Sarachik, 2000: Rayleigh friction, Newtonian cooling, and the linear response to steady tropical heating. *J. Atmos. Sci.*, **57**, 1937–1957, doi:10.1175/1520-0469(2000)057<1937:RFNCAT>2.0.CO;2.

Zhang, C., D. S. Nolan, C. D. Thorncroft, and H. Nguyen, 2008: Shallow meridional circulations in the tropical atmosphere. *J. Climate*, **21**, 3453–3470, doi:10.1175/2007JCLI1870.1.